Sensors and Actuators B 255 (2018) 3616–3622

Contents lists available at ScienceDirect

Sensors and Actuators B: Chemical

journal homepage: www.elsevier.com/locate/snb

Research paper

Feedback control system for large scale 2D digital microfluidic platforms

Chunqiao Li, Kaidi Zhang, Xubo Wang, Jian Zhang, Hong Liu, Jia Zhou *

ASIC and System State Key Lab, Department of Microelectronics, Fudan University, Shanghai 200433, People's Republic of China

ARTICLE INFO

Article history:
Received 10 June 2017
Received in revised form 8 September 2017
Accepted 12 September 2017
Available online 14 September 2017

Keywords:
Microfluidics
Electro-wetting
Two-dimension
Feedback control

ABSTRACT

As a promising candidate of point-of-care devices (POC), digital microfluidic (DMF), driven by the electrowetting-on-dielectric (EWOD), has been developed quickly in recent years. However, flourishing functions require more controlled electrodes, *i.e.*, a large-scale EWOD. Limited to cost, complexity and flexibility, existing control techniques lack strength in meeting the need of controlling increasing number of electrodes. Here, inspired by the active matrix electrowetting-on-dielectric (AM-EWOD), we present a "direct-address based on cross-control" (DACC) method, which can easily realize N + M pins controlling N × M electrodes and guarantee the control flexibility meanwhile. Moreover, combining with impedance detection technique, we set up a cheap and portable cyberphysical system. The system's software, written in JAVA, has a user-friendly interface and can sense all sites of the DMF in real-time and auto-design routes for droplets to bypass barriers. This novel integrated digital microfluidic system shows great potential for developing low-cost, portable, and automated EWOD DMFs in large-scale.

1. Introduction

Based on manipulation of microliter or nanoliter droplets, digital microfluidic biochips have taken up some biomedical applications that require more complicated operations and high flexibilities, which the traditional continuous-flow cannot handle [1,2]. For instance, Srinivasan et al. [3] presented a fully integrated and reconfigurable droplet-based "digital" microfluidic lab-on-a-chip for clinical diagnostics on human physiological fluids. Ng et al. [4] performed a complete sample preparation on a digital microfluidic chip for the detection of rubella infection and immunity. Among the numerous driving mechanisms in digital microfluidic devices, the technique, electrowetting-on-dielectric (EWOD), is given high expectations due to its excellent flexibility and best functionality [5].

With more and more functions integrated, digital microfluidic biochips, driven by EWOD, step towards 2D and large-scale [6–9]. When designing a 2D EWOD DMF, two fundamental questions need to be solved properly. One is how to control the increasing number of electrodes effectively. In most reports on EWOD, controlling droplets were implemented in a passive manner. The earliest passive control is of direct-address that actuation signals are directly applied on individual electrode upon the droplet manipulation. However, the expanding number of electrodes limited such technique. The second passive-EWOD's control technique is of cross-reference presented by Fan et al. [10,11]. In spite of successfully reducing the number of control pins from N × M to N + M, this new driving mechanism still lives on the edge of EWOD DMFs since it is short of flexibility in controlling droplets individually. The latest passive control technique for EWOD is the broadcast-address suggested by Zhao et al. [12]. Frankly a pity, this sort is assay-specific in majority, *i.e.* the droplets' operations are pre-determined, which violates the reconfigurable merit of 2D EWOD DMF. Lately, active matrix electrowetting-on-dielectric (AM-EWOD) based on thin film transistors (TFT) emerged, which can easily manipulate thousands of individual electrodes. Kalsi et al. [7] used this technology realizing rapid and sensitive detection of antibiotic resistance. However, judging from the present condition, this integrated product is customized, whose cost may be prohibitive.

The other issue is how to schedule routes for droplets. As we know, this is such a complex work that not only the experimental procedures, but also on-chip faults and barriers should be considered. Computer-aided design (CAD) is an inevitable choice. A number of techniques used in VLSI circuits have been proposed to solve droplet-routing problem [1,8,13–15]. However until now, to our best knowledge, except that K. Hu et al. [16], M. Ibrahim et al. [17] and J. Gao et al. [18] presented experimental demonstra-

* Corresponding author.
E-mail address: jia.zhou@fudan.edu.cn (J. Zhou).

http://dx.doi.org/10.1016/j.snb.2017.09.071
0925-4005/

Table 1
Comparison of direct-address, cross-reference, broadcast-address, TFT, and DACC.

Electrode control technique	Actuation signal	Integrating TFT	Control pins	Control flexibility	Cost
direct-address	T or B[a]	No	N × M[c]	Very high	Up to control pins
cross-reference	T & B[b]	No	N + M	Very low	Low
broadcast-address	T or B	No	≤N × M	Low	Low
TFT	T or B	Yes	N + M	High	Specific design and manufacture, possibly high
DACC	T or B	No	N + M	High	Low

[a] T or B denotes that only one set of actuation signal is needed for controlling droplets. The actuation signal can be applied to the patterned top electrode if the bottom electrode is grounded or vice versa.
[b] T & B denotes that two sets of actuation signal are needed for controlling droplets. One set is connected to the patterned top electrode while the other to the patterned orthogonal bottom electrode.
[c] N and M mean that a 2D N × M EWOD array has N rows and M columns.

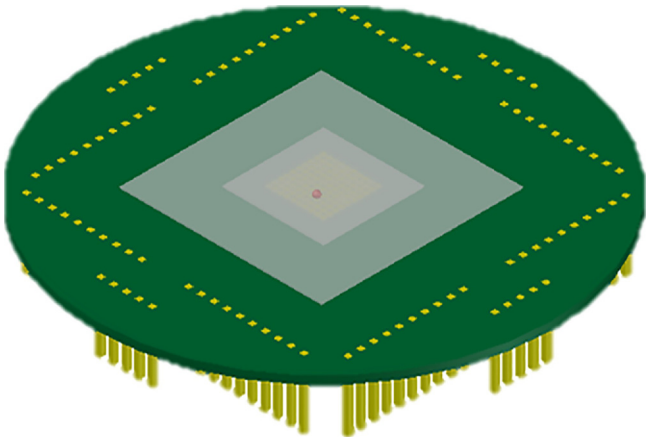

Fig. 1. Schematic of our designed PCB based DMF. One hundred male heads connecting with one hundred electrodes surround the core EWOD region.

tions, almost other researchers, who idealize the important details, *e.g.* error detection and hardware/software interface, are staying at modeling and simulation. Moreover, K. Hu's and J. Gao's methods lacked of scalability for their sensing hardware's complexity, while M. Ibrahim's limited in image-processing.

In this paper, we mainly focus on breaking through the above two dilemmas. A cyberphysical system, which adopts a novel passive electrode-control technique named "direct-address based on cross-control" (DACC) and utilizes CAD algorithm to realize autorouting droplets in concerns of on-chip barriers, will be introduced. The system's hardware and software are both capable of expanding to larger-scale 2D DMF. The EWOD chip is built on a double-layer printed circuit board (PCB), which comprises of 10 × 10 electrodes. As shown in Fig. 1, one hundred male heads connecting with one hundred electrodes surround the core EWOD region. Table 1 lists the actuation signal, integrating TFT, control pins, control flexibility, and cost for direct-address, cross-reference, broadcast-address, TFT, and DACC. The comparison shows that the DACC is a good candidate for passive EWOD applications, providing respectable simplicity and flexibility at low costs. The rest of paper is organized as follows. Section 2 describes the process of fabricating a PCB-EWOD device, DACC working principle and the adopted droplet transportation algorithm. The system configuration including hardware and software is shown in Section 3. Experimental details and discussions are presented in Section 4. Section 5 concludes the paper.

2. EWOD device and droplet transportation

2.1. EWOD device on double-layer PCB

A PCB, besides low-cost and maturity, is quite convenient to accomplish electrical access from the inner electrodes to the external control circuit because its drilled via can have Cu-electroplated inner walls. There only need several simple procedures to obtain a PCB-based EWOD device. As shown in Fig. 2, a two-layer PCB substrate with conductive polymer filled via was first mechanically polished by grinding papers, which was beneficial for eliminating the effect of grooved surfaces [19,21]. After cleaning, 300 nm Al was deposited and patterned into a two-dimensional electrode array. Then 2 μm SU-8 (SU-8 2002, MicroChem) as the dielectric layer and 200 nm Teflon® AF1600 solution (Du Pont, 2 wt%) as the hydrophobic layer were spun. At last, the top glass, coated with 200 nm transparent ITO as the upper electrode and 200 nm Teflon® as the hydrophobic layer, was set above the EWOD-PCB substrate by about 150 μm double-sided tape. The EWOD chip has 1.74 mm × 1.74 mm square electrodes. The control circuit can access the two-dimensional array through the connection lines on the PCB-EWOD chip substrate.

2.2. DACC working principle

Since the most successful and applicable control technology of electrodes for large-scale 2D DMF is AM-EWOD until now, based on deep understanding of it, we found that the core of AM-EWOD is the vital function of integrating TFTs. As known, TFT is a logic electronic switch whose drain will be connected to the source when the gate is applied a proper potential. The logical relationship of a TFT is same as an AND circuit. Inspired by this, through incorporating AND circuits, we present the new passive electrode-control technique – "direct-address based on cross-control" (DACC) – for somewhere integrating TFTs is not available. This technique can realize similar effects as AM-EWOD and theoretically control as many individual electrodes as required if the driving capability is enough. We verify the concept on an EWOD with 10 × 10 grids. Thus, only 10 row control pins and 10 column control pins are needed to address all sites.

We arrange 2-input AND gates in a 10 × 10 array and then connect each row/column control pin with each row/column AND gates' first/second input terminals, *e.g.* the 1th row control pin will be connected to the 1th row AND gates' first input terminals. The 10 + 10 control pins generate 10 × 10 control signals. To address a (n, m) site, applying a high potential on the n^{th} row control pin and the m^{th} column control pin is enough.

Therefore, DACC significantly increases flexibility compared with the previous cross-reference method. Moreover, as the commercial AND chip is economical and well packed, this technique is in low-cost and easy to assemble by oneself in lab.

2.3. Droplet route on EWOD device

Typically, a large-scale 2D EWOD digital microfluidic biochip has a set of electrodes that allow droplets moving on arbitrary paths, depending on the freely programmable electrode activation sequences. Among CAD algorithms for finding paths in rectangu-

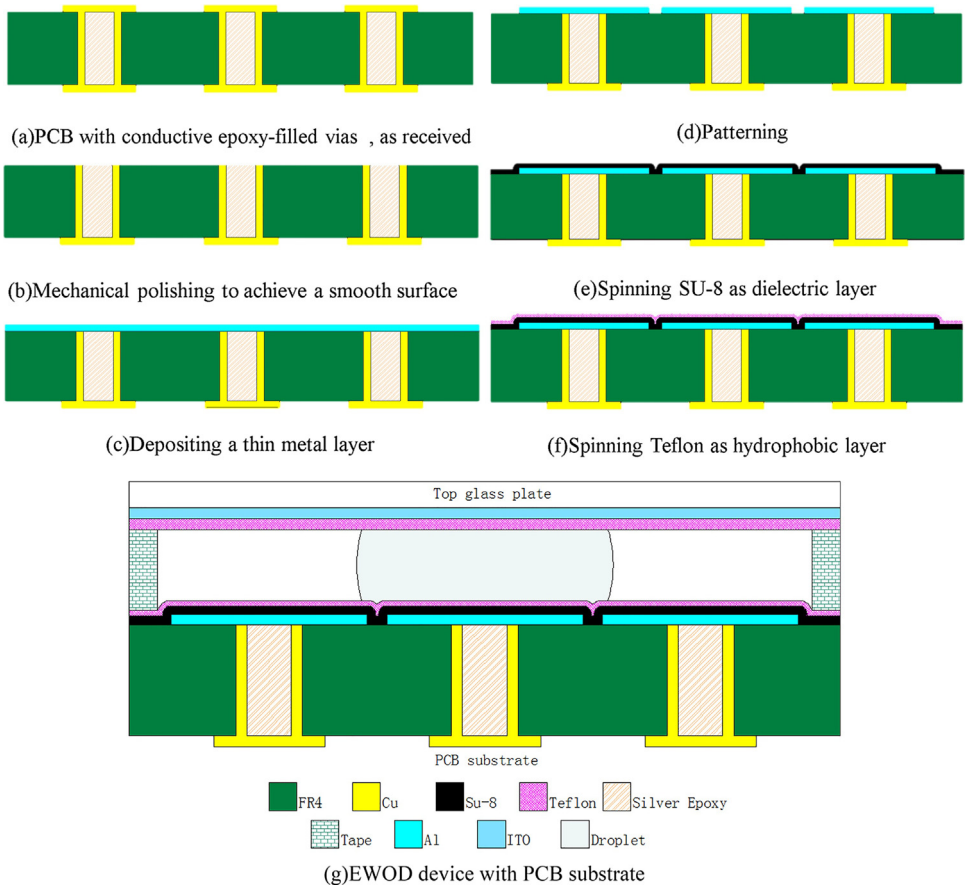

Fig. 2. Process of EWOD device on PCB substrate. (a) Specially engineered PCB with conductive epoxy-filled via. (b) Polishing with grinding papers. (c) Deposition of Al layer though PVD (ASC-4000-C4 Type L, ULVAC, Japan). (d) Photolithography and wet-etching of Al electrodes. (e) Spinning, baking and exposure of dielectric layer SU-8. (f) Spinning and baking of hydrophobic layer Teflon. (g) PCB-EWOD chip with double-sided tape as spacer between PCB and top electrode.

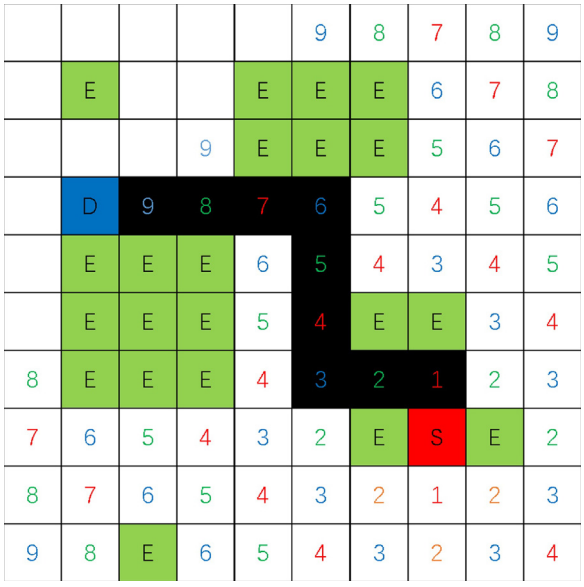

Fig. 3. Lee algorithm finds an appropriate path in a 10 × 10 cells graph.

lar grids, Lee algorithm is the most widely used one, which can find connection between two terminals if it exists and guarantee the minimum path. As shown in Fig. 3, the Lee algorithm finds an appropriate path, *i.e.* the black cells, from the starting point, *i.e.* the red cell labelled 'S', to the destination, *i.e.* the blue cell labelled 'D', in a 10 × 10 cells graph. The cells labelled 'E' represent detected error sites, including barriers or faults.

Compared with algorithms' quick routing capabilities (less than 20 ms in ref. [13]), droplet movement on an EWOD chip is quite slow, typically 8 Hz on glass-substrate DMFs [20] and 7.8 mm/s (about 5 Hz) on PCB-substrate DMFs [21]. In this paper, we ignore the time-consuming differences among algorithms and employ the Lee algorithm to route droplets with real-time feedback from error detection.

3. System configuration

The system comprises of four parts: impedance value extracting circuit, DACC circuit, a microcontroller (Arduino Mega2560, Smart-Projects, Italy) and a host PC that runs a GUI application.

3.1. System hardware

Hardware for the real-time feedback control has been realized through three double-side PCBs of 27cm × 23cm × 1.6mm, as shown in Fig. 4(a). Devices on the bottom board and middle board are components of the DACC circuit. The bottom board consists of 25 small surface mount chips (74HC08D, quad 2-input AND gate, Philips Semiconductors). These chips are regulated by the microcontroller, of which 20 pins (10 row pins and 10 column pins) can cross-control 100 signals. The middle board comprises 100 solid-state relays (SSR, AQH2223, Panasonic Corporation), each of which is managed by an AND gate output signal. When a high-level signal applies across a SSR's control terminal, the SSR will switch the

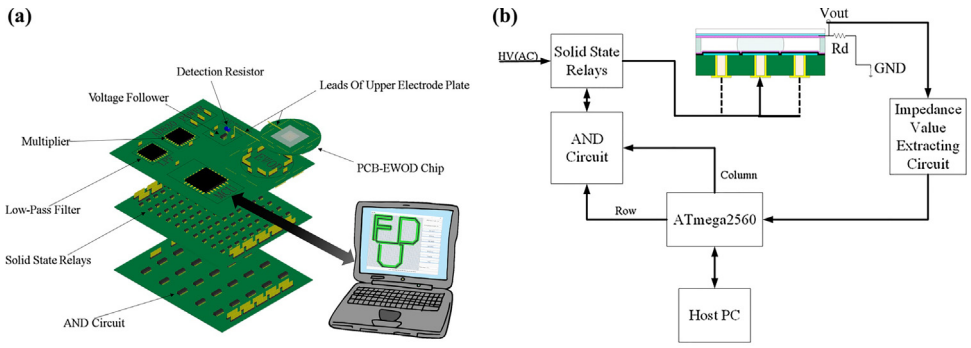

Fig. 4. Schematic of droplet actuation and detection system. (a)System hardware mimic diagram. (b)Flow of signal among circuit components.

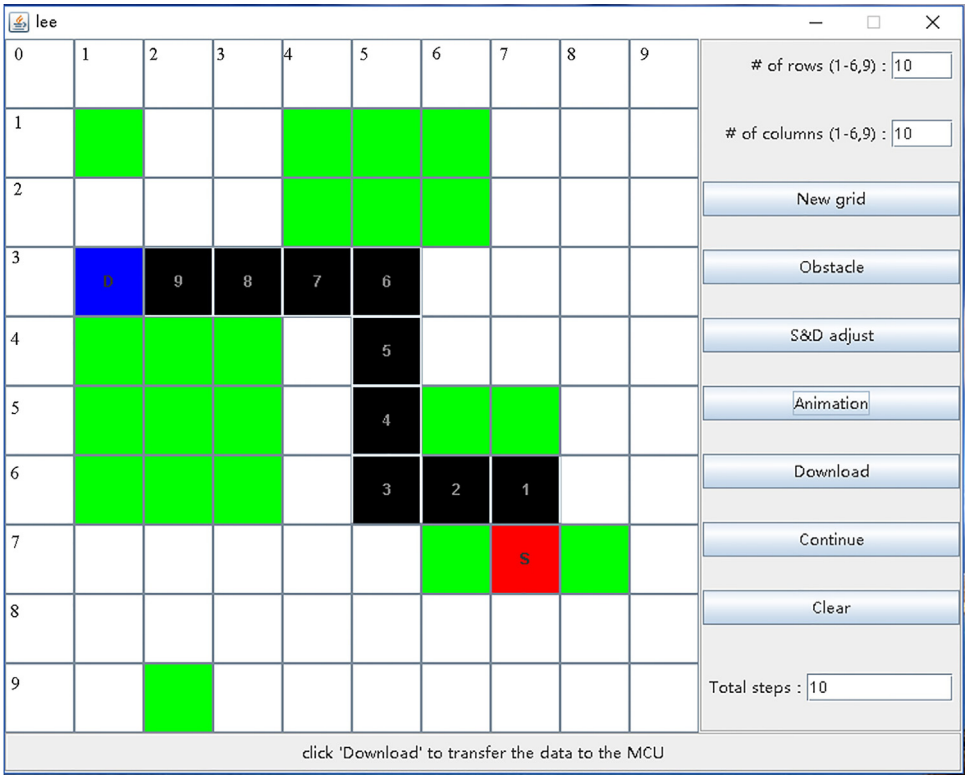

Fig. 5. Screenshot of the DMF control software. Obstacles of the DMF can be set manually or detected automatically. The auto-designed droplet route could be downloaded into the microcontroller by clicking the "Download" button.

AC power to the electrode. The top board is the core of the whole system, on which the microcontroller, the PCB-EWOD chip and the impedance value extracting circuit are all installed. The actuation and feedback control algorithm can be easily programmed with a PC and downloaded into the microcontroller through on-board USB. Communications between the host pc and the microcontroller are using the same USB. Fig. 4(b) shows the flow of signal among circuit components. The dotted lines stand for SSRs' leakage currents.

The impedance value extracting circuit houses a slide-detecting resistor R_d, a voltage follower, a multiplier and a low-pass filter, the working principle of which resembles reference [22–24]. The EWOD chip's impedance detection signal V_{out} will be firstly delivered to the voltage follower in order to match circuit impedance. Then the tracked signal will be added to the multiplier to multiply itself. The low-pass filter is used to filter the multiplier's product, which generates a DC signal corresponding to the EWOD device's impedance. Finally, through an analog to digital converter (ADC, 10-bit resolution) of the microcontroller, the DC signal is acquired and a feedback control loop forms up. A cut-off DC value is set for defining the faults and barriers. Once the DC signal is beyond the threshold, the software on the host PC will regard the corresponding site as a fault or barrier.

3.2. User interface

Fig. 5 shows a screenshot of the Java application we designed for DMF control. The application named "lee" can not only transmit a sequence of bit vectors representing electrode actuations to the microcontroller but also receive sites' information from the microcontroller.

The number of row and column of electrodes can be set by the user as necessary. This control software permits either manual or automatic errors scanning of the device. For instance, after setting rows and columns of the device and clicking "New grid" and "Obstacles", the user can click on cells to turn them green or not. It should be noted that in Fig. 5, green cells are selected by the user for sym-

bolizing errors; the red cell represents a starting point of a droplet while the blue stands for a destination. Once the error positions, the droplet starting points and destinations are defined, by clicking the "Animation" button an appropriate route (black cells) will be instantly figured out based on the Lee algorithm. To avoid the positions of errors intelligently, the starting point and destination are given by the software firstly, and could be dragged arbitrarily later. If the user clicks the button "Download", the electrode activation sequence will be downloaded into the microcontroller immediately. Almost simultaneously, the droplet on the chip would move along the auto-designed route.

What is more, every time clicking the "Obstacles" button, the control algorithm in the microcontroller will scan the route that the droplet has just passed and deliver error sites' positions to the host PC. The control software lets green cells labelled "E" represent these sites. Note that, if it is the first time clicking the button "Obstacles" after launching the software, the microcontroller will scan the whole chip. The button "Continue" is used to start next time transportation of the droplet, which will retain the last time error sites' information and exchange the starting and ending points. If the user clicks the "Clear" button, the software will return to the initial state. Furthermore, there are two message boxes, one displaying the total steps of the auto-designed route and the other at the bottom of the interface prompting the next operation. Further details about software's elementary operations are provided in video S1.

The architecture of the system shows great flexibility in hardware and software. On the aspect of hardware, the electrode number on the PCB can be easily increased or decreased as needed, which only requires the DACC circuit to change a little, *i.e.* increasing or decreasing the number of control pins, AND gates, and SSRs. As to the impedance value extracting circuit, no matter how many electrodes there are, the obstacle detection is always available. On the aspect of software, user has the right to adjust number of the row and the column, and set up the forbidden electrodes by obstacle detection automatically or auxiliary manual operation in-time.

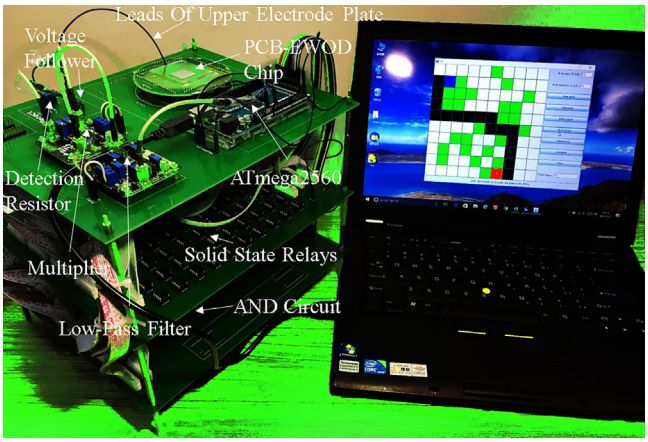

Fig. 6. Prototype photo of the low-cost feedback control system.

4. Experimental results and discussions

4.1. Addressing method verification

The whole prototype system is shown in Fig. 6, which occupies a space same as a laptop computer. Of course, there remains lots of room to optimize. The custom pogo-pin connectors enable plug-pull between PCB-EWOD chip and the core board.

DACC circuit was put to test by planning "S" shaped route for a droplet and manipulating multiple droplets in an air environment. Firstly, we applied an AC signal of 78 Vrms with a frequency of 1 kHz to the system. Then through the Arduino IDE 0023, the designed routes were downloaded to the microcontroller and the SSRs' switch rate was adjusted to 1 Hz in the microcontroller. A digital HD video camera was used (HDR-CX110, Sony) to record droplets' performances. Parameter tuning is precise, *e.g.* droplet

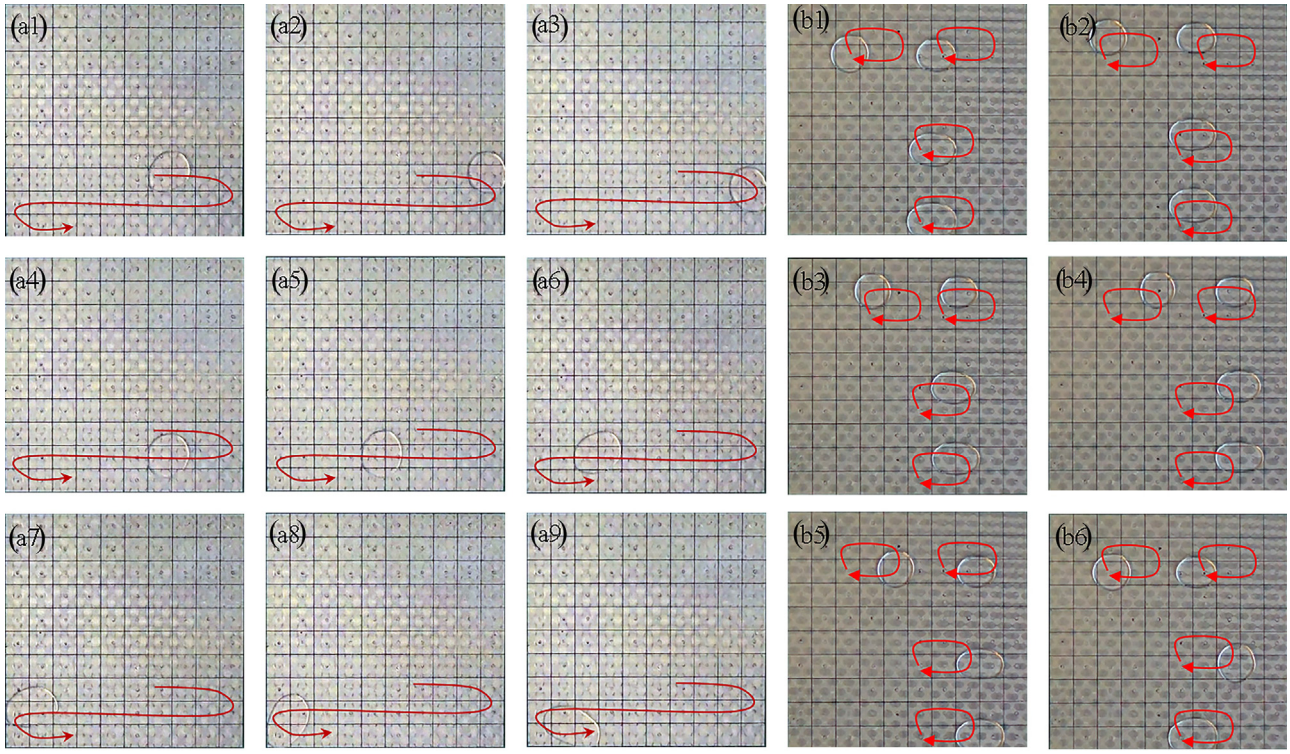

Fig. 7. "S" shaped route for a droplet and manipulation of multiple droplets. Pictures (a1–a9) were taken at 1 s, 4 s, 5 s, 8 s, 10 s, 13 s, 14 s, 15 s and 17 s of video S2, while pictures (b1–b6) were taken at 25 s, 28 s, 30 s, 31 s, 33 s and 38 s of video S3.

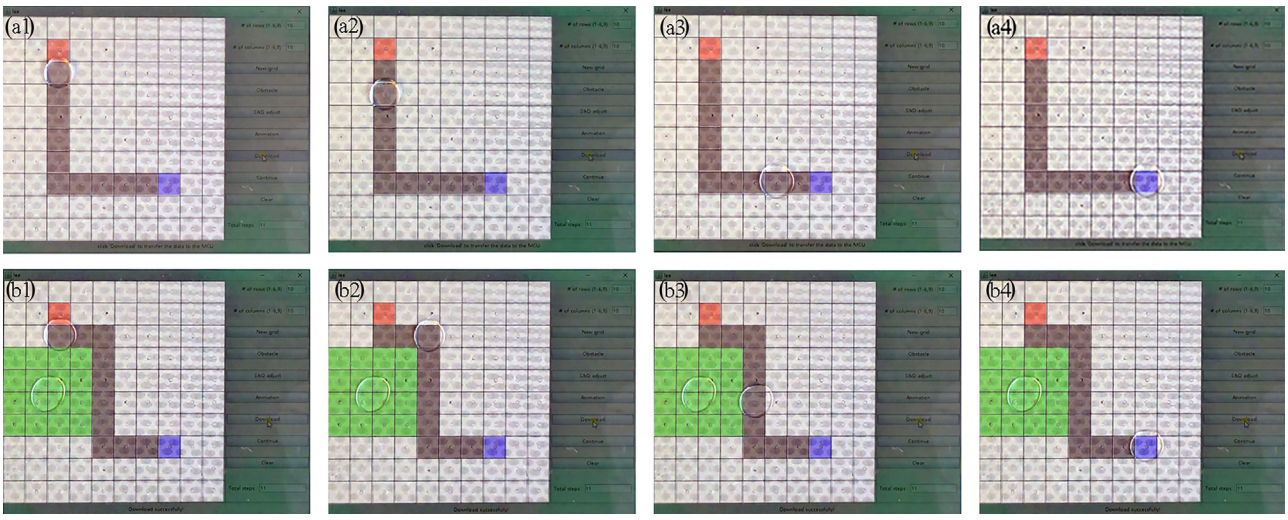

Fig. 8. A droplet avoids a barrier. (a1–a4) The droplet moves straightway from the starting point to the destination when there was no barrier on. (b1–b4) After sensing a barrier blocking the previous route, the software figures out another path for the droplet.

size was guaranteed by on-chip droplet dispensing [25] or a pipette (in this work), while actuation signal could be tuned by a signal generator and a high voltage amplifier.

Fig. 7 shows the addressing method verification result. Fig. 7(a1–a9) exhibit an 1 μL deionized water (DI) droplet moving along a "S" shaped route, which were taken at 1s, 4s, 5s, 8s, 10s, 13s, 14s, 15 s and 17 s of video S2. As shown, the droplet smoothly moved from the 7th row to the 9th row. That droplet's velocity can be tuned 17mms^{-1} was observed by heightening the SSR's switch rate (see video S3). Fig. 7(b1–b6) exhibit multiple droplets manipulating, which were taken at 25s, 28s, 30s, 31s, 33 s and 38 s of the video S3. Four droplets spun clockwise at four six-electrode regions. Droplets' spinning direction is not fixed, which can be altered when writing the control algorithm in the microcontroller.

As expected, through the DACC circuit, either a droplet or multiple droplets can be moved successfully. Our PCB-substrate chip's droplet achieved even comparable velocity with the glass-substrate DMF's. Moreover, when manipulating multiple droplets, no obvious electrode interference was observed, which illustrates that the DACC circuit far exceeds the conventional cross-reference method in control flexibility. This novel passive electrode-control technique demonstrates the capability applicable for large-scale 2D EWOD DMFs.

4.2. Feedback control

A series of experiments was implemented to test the auto-designed route's capability of barriers avoiding. To begin with the first experiment, we set the detection threshold that was based on the previous detection experiments, applied an AC signal of 78 Vrms with a frequency of 1 kHz to the system and adjusted the SSRs' switch rate to 1 Hz. Next, a 1 μL DI droplet was put on a dry chip. The starting point and destination were set on the custom software. Finally, after clicking the "Animation" button and subsequently recording the auto-designed route, we clicked the "Download" button to observe the droplet's movement.

At the second experiment, we put a 1 μL DI droplet on the above auto-designed route as a barrier and clicked the "Obstacle" button. The same starting point and destination were chosen. Next, we clicked the "Animation" button again and recorded the new generated route. After clicking the "Download" button, the droplet's new movement was observed.

Fig. 8 exhibits the above two experiment results, *i.e.* the whole process of a droplet avoiding a barrier. For comparison, the PCB-EWOD chip's optical images were composited with the software interface. Fig. 8(a1–a4), taken at 21s, 23s, 29 s and 32 s of video S4, show that the droplet moves straightway from the starting point to the destination when there was no barrier on, *i.e.* a dry chip. Fig. 8(b1–b4), taken at 55s, 57s, 59 s and 65 s of video S5, show that after a barrier detected and blocking the previous route, the software figures out another path for the droplet.

Droplet moving almost simultaneously began by clicking "Download". As expected, when the chip was dry, the software did not find any barrier on, so it recommended an "L" shaped route (Fig. 8(a1–a4)). When a barrier existed, the software marked the constraint area in milliseconds and figured out another path (Fig. 8(b1–b4)). In these auto-routing processes, the Lee algorithm guaranteed the minimum paths. This 100% agreement between the software and the PCB-EWOD chip's performances shows a large potential for developing automated EWOD DMFs.

5. Conclusions

We set up a prototype system with hardware and software potentially applicable for large-scale 2D EWOD DMFs with great flexibility. Hardware for direct-address based on cross-control (DACC) and impedance detecting feedback control on a passive EWOD DMF was successfully designed and implemented. Through DACC circuit, multiple droplets could be manipulated simultaneously without interference. Our user-friendly software works fine. An example of auto-routing and barriers avoiding was exhibited. Such all-electronic feedback control method to escort on-chip droplets enables a portable and intelligent design of DMF systems. The system for the tested example of PCB-based 10 × 10 EWOD device is in low-cost of below $130.

Acknowledgement

This work was supported by the National Science Foundation of China with Grant No. 61674043.

Appendix A. Supplementary data

Supplementary data associated with this article can be found, in the online version, at http://dx.doi.org/10.1016/j.snb.2017.09.071.

References

[1] Y. Zhao, K. Chakrabarty, Design and Testing of Digital Microfluidic Biochips, Springer, New York, Heidelberg, Dordrecht, London, 2013.
[2] F. Mugele, J.-C. Baret, Electrowetting: from basics to applications, J. Phys. Condens. Matter. 17 (2005) R705–R774.
[3] V. Srinivasan, V.K. Pamula, B.F. Richard, An integrated digital microfluidic lab-on-a-chip for clinical diagnostics on human physiological fluids, Lab Chip 4 (2004) 310–315.
[4] A.H.C. Ng, M. Lee, K. Choi, A.T. Fischer, J.M. Robinson, A.R. Wheeler, Digital microfluidic platform for the detection of rubella infection and immunity: a proof of concept, Clin. Chem. 61 (2) (2015) 420–429.
[5] E. Samiei, M. Tabrizian, M. Hoorfar, A review of digital microfluidics as portable platforms for lab-on a-chip applications, Lab Chip 16 (2016) 2376–2396.
[6] B. Hadwen, G.R. Broder, D. Morganti, A. Jacobs, C. Brown, J.R. Hector, Y. Kubota, H. Morgan, Programmable large area digital microfluidic array with integrated droplet sensing for bioassays, Lab Chip 12 (2012) 3305–3313.
[7] S. Kalsi, M. Valiadi, M.-N. Tsaloglou, L. Parry-Jones, A. Jacobs, R. Watson, C. Turner, R. Amos, B. Hadwen, J. Buse, C. Brown, M. Sutton, H. Morgan, Rapid and sensitive detection of antibiotic resistance on a programmable digital microfluidic platform, Lab Chip 15 (2015) 3065–3075.
[8] M. Alistar, Towards droplet size-aware biochemical application compilation for AM-EWOD biochips, in: Presented in Part at 2015 Symposium on Design, Test, Integration and Packaging of MEMS and MOEMS(DTIP), Montpellier, France, April, 2015.
[9] D. Grissom, A field-programmable pin-constrained digital microfluidic biochip, in: Presented in Part at 2013 50th ACM/EDAC/IEEE Design Automation Conference (DAC), Austin, USA, June, 2013.
[10] J. Gong, Two-dimensional digital microfluidic system by multi-layer printed circuit board, in: Presented in Part at 18th IEEE International Conference on Micro Electro Mechanical Systems, 2005. MEMS, 2005, Miami, USA, January, 2005.
[11] J. Gong, Portable digital microfluidics platform with active but disposable lab-on-chip, in: Presented in Part at the 17th IEEE International Conference on Micro Electro Mechanical Systems. Maastricht MEMS 2004 Technical Digest, Maastricht, Netherlands, January, 2004.
[12] Y. Zhao, T. Xu, K. Chakrabarty, Broadcast electrode-Addressing and scheduling methods for pin-constrained digital microfluidic biochips, IEEE Trans. Comput. Aided Des. Integr. Circuits Syst. 30 (2011) 986–999.
[13] D. Grissom, C. Curtis, S. Windh, C. Phung, N. Kumar, Z. Zimmerman, K. O'Neal, J. McDaniel, N. Liao, P. Brisk, An open-source compiler and PCB synthesis tool for digital microfluidic biochips, Integr. VLSI J. 51 (2015) 169–193.
[14] J.H. Hoel, Some variations of lee's algorithm, IEEE Trans. Comput. c-25 (1976) 19–24.
[15] F. Rubin, The lee path connection algorithm, IEEE Trans. Comput. c-23 (1974) 907–914.
[16] K. Hu, Fault detection, real-time error recovery, and experimental demonstration for digital microfluidic biochips, in: Presented in Part at 2013 Design, Automation and Test in Europe Conference and Exhibition (DATE), Grenoble, France, March, 2013.
[17] M. Ibrahim, K. Chakrabarty, Efficient error recovery in cyberphysical digital-microfluidic biochips, IEEE Trans. Multi-Scale Comput. Syst. 1 (2015) (2015) 46–58.
[18] J. Gao, X. Liu, T. Chen, P.-In Mak, Y. Du, M.-I. Vai, B. Lin, R.P. Martins, An intelligent digital microfluidic system with fuzzyenhanced feedback for multi-droplet manipulation, Lab Chip 13 (2013) 443–451.
[19] Z. Wang, Y.-P. Zhao, Wetting and electrowetting on corrugated substrates, Phys. Fluids 29 (2017) 067101.
[20] M.G. Pollack, Electrowetting-based Microactuation of Droplets for Digital Microfluidics, PhD Thesis, Duke University, 2001.
[21] J. Gong, C.-J. Kim, Direct-referencing two-dimensional-array digital microfluidics using multilayer printed circuit board, J. Microelectromech. Syst. 17 (2008) 257–264.
[22] S. Sadeghi, H. Ding, G.J. Shah, S. Chen, P.Y. Keng, C.-J. Kim, R.M. van Dam, On chip droplet characterization: a practical, high-sensitivity measurement of droplet impedance in digital microfluidics, Anal. Chem. 84 (2012) 1915–1923.
[23] S.C.C. Shih, R. Fobel, P. Kumar, A.R. Wheeler, A feedback control system for high-fidelity digital microfluidics, Lab Chip 11 (2011) 535–540.
[24] R. Fobel, C. Fobel, A.R. Wheeler, DropBot: an open-source digital microfluidic control system with precise control of electrostatic driving force and instantaneous drop velocity measurement, Appl. Phys. Lett. 102 (2013), 193513-1–193513-4.
[25] W. Wang, J. Chen, J. Zhou, An electrode design for droplet dispensing with accurate volume in electro-wetting based microfluidics, Appl. Phys. Lett. 108 (2016) (243701-1-243701-5).

Biographies

Chunqiao Li is currently pursuing the master degree with the State Key Laboratory of ASIC and Systems, School of Microelectronics, Fudan University. His research interest focuses on Biochemical application based on microfluidic technology, EDA (IC, Digital Microfluidic) and Smart system.

Kaidi Zhang is currently pursuing the doctor degree with the State Key Laboratory of ASIC and Systems, School of Microelectronics, Fudan University. His research interest focuses on digital microfluidic devices and their applications in biology.

Xubo Wang is currently pursuing the doctor degree with the State Key Laboratory of ASIC and Systems, School of Microelectronics, Fudan University. His current research focus on the design and optimization of ultrasonic sensors.

Jian Zhang is currently pursuing the master degree with the State Key Laboratory of ASIC and Systems, School of Microelectronics, Fudan University. His research interest focuses on smartphone-based electrochemical analysis system.

Hong Liu is currently pursuing the master degree with the State Key Laboratory of ASIC and Systems, School of Microelectronics, Fudan University. His research interest focuses on the design and optimization of humidity sensors.

Jia Zhou received the Ph.D. degree from Fudan University in 2004. She is currently a Professor with the State Key Laboratory of ASIC and Systems, School of Microelectronics, Fudan University. Her research interests are in nano/microfluidics, MEMS/NEMS-based chemical, biochemical and biomedical sensors, and their applications.